Assessment of Power Generation Capability of Doubly-Salient PM Generator

Bulent Sarlioglu
Toshiba International Corporation
Research and Development Engineering Department
13131 W. Little York Rd. Houston, TX 77041
bulent.sarlioglu@tic.toshiba.com

Thomas A. Lipo
University of Wisconsin - Madison
Electrical and Computer Engineering Department
1415 Engineering Dr. Madison, WI 53706
lipo@engr.wisc.edu

Abstract – **In this paper, the characterization of the power production capability of the DSPM generator under loaded conditions will be fully explored by using relevant power electronic circuit implementations. The ac output of the DSPM generator can easily be rectified to power a dc load. In certain applications, the requirement is for constant dc rectifier current, while in some applications dc voltage should be constant. The required rectification can be done by using a variety of power electronics circuits. A diode bridge rectifier with constant current and constant voltage output, and a PWM boost controller with a hysteresis current controller are the implementations of interest. In the case of an actively switched converter, semiconductor devices are used to shape the current, and hence provide a controlled power transfer.**

I. INTRODUCTION

New doubly salient ac machines in which the field is excited by either stationary or rotating magnets have recently been undergoing development at the University of Wisconsin-Madison [1-7]. The physical description and modeling of a doubly salient permanent magnet (DSPM) generator version of this new concept is given in References 1-4. In References 2 and 3, the power output capability of the DSPM generator is compared with the switched reluctance and induction machine and determined to be superior. For example, by using sizing equation, it is shown that the DSPM generator has 40 % more power production capability with respect to an induction machine for the same volume, speed, and electrical loading. In Reference 4, a nonlinear analysis based on cubic spline theory using detailed finite element (FEM) analysis is developed. It has been shown that design of the generator and power electronics can be made more accurate by combining FEM analysis and nonlinear analysis techniques than simply using first order approximations of the back-emf and inductance terms.

In this paper, the results to assess the power generation capability of the DSPM generator by using various power electronic rectification techniques will be presented.

II. BRIDGE RECTIFIER WITH CONSTANT DC LINK CURRENT

In this implementation a simple diode bridge rectifier is used to convert the ac output power of the DSPM generator into dc power. A sufficiently large inductor is placed in series with a resistance to achieve a constant current as shown in Fig. 1. Fig. 2 shows the waveforms obtained at 3000 rpm and 0.49 ohm. The dc link current loading is 30.8 A.

A. *Output Characteristic of Generator*

Various tests were carried out for different load values and speed ranges to study the output characteristics of the generator by using bridge rectifier with constant dc link current. Three inductors and a resistive load are connected in series. Each inductor is 30.65 mH and has an internal resistance of 0.15 ohm. A Quad Tech 7600 precision RLC meter was used to measure the inductance and resistance seen by the rectifier to achieve an accurate reading of total inductance and resistance values. The constant current output characteristic of the DSPM generator through a bridge rectifier is shown in Fig. 3 and Fig. 4.

It should also be noted from Fig. 2 that the commutation time in which two rectifier diodes are supplying constant dc current is critical for shaping the characteristic of the DSPM generator in this case. In another words, the dc output voltage is zero during the commutation, since the output of the DSPM generator is short-circuited. Hence, the inductance value of the DSPM generator can be tailored by design to achieve the desired output voltage characteristic with respect to the desired current. As the inductance gets smaller, which requires a larger airgap and fewer number of turns, this commutation time will be smaller, yielding a higher voltage output.

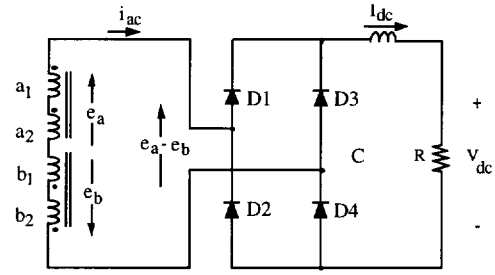

Fig. 1 Rectification with constant dc current.

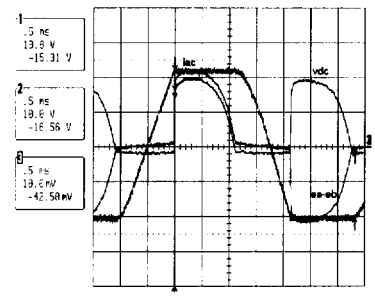

Fig. 2 Experimental results: (Traces: Voltages 10 V/div, current 20 A/div)

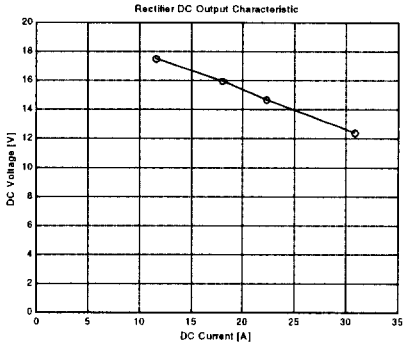

Fig. 3 DC current and DC voltage relationship for constant current rectifier

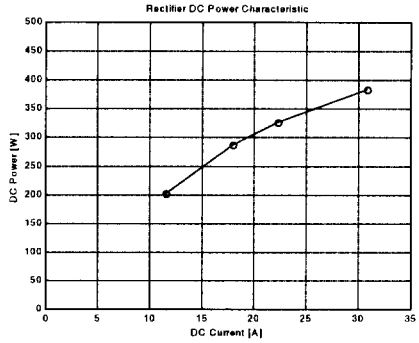

Fig. 4 DC current and DC power relationship for constant current rectifier

B. Comparison of Experimental Results with Simulations

Experimental results have been compared by using first order approximation and nonlinear simulation results. Diode voltage drops (a total of 3.5 V) are included in the simulations and the dc link current and rotor speed are set to same as those of the experiment. These results are shown in Fig. 5.

In the case of a first order approximation, the dc power output and commutation time are calculated 664 W and 410 μs, respectively. Considering the dc power output and commutation time from the experimental results were 384 W and 610 μs respectively, the results are not as accurate as had been obtained from the nonlinear analysis. Since a first order approximation analysis does not take into account the effect of armature reaction, the inductances used in the simulation are not very accurate. Also, the back emf voltage used in first order approximation was overestimated by using a rectangular waveform. This rectangular back emf voltage causes a faster rate of change of phase current during the commutation which tends to shorten the commutation time.

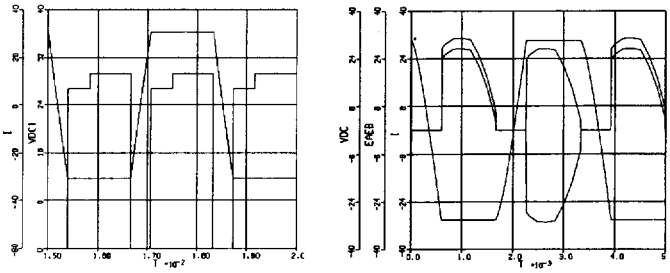

Fig. 5 **Left:** First Order Approximation Simulation Results: Rectified voltage v_{dc1} and ac current i. **Right:** Nonlinear Simulation Results: Rectified voltage v_{dc}, voltage e_a-e_b (v_{ac}), and ac current

A simulation was also done using the nonlinear results obtained from a finite element analysis to improve the accuracy of the modeling [4]. DC output power is calculated as 384 W experimentally, while it is 425W from the simulation. The difference is 10 %. Also, the commutation times of the current from the experiment and simulation are 610 μs and 700 μs, respectively. Therefore, a good correlation is also achieved in this portion of the waveform.

The results from experiment and simulations are tabulated in Table 1. It can be concluded that the nonlinear simulation results are in better agreement than the first order approximation simulation.

TABLE I
COMPARISON OF EXPERIMENTAL, FIRST ORDER APPROXIMATION RESULTS, AND NONLINEAR SIMULATION.

Results From	DC Output Power (W)	DC Output Power (pu)
Experiment	1400	1.00
Nonlinear Sim.	1320	0.94
First Order App. Sim.	1710	1.22

III. BRIDGE RECTIFIER WITH CONSTANT DC OUTPUT VOLTAGE

In a similar test to that in the previous section, the output voltage of the bridge rectifier was kept constant by a sufficiently large capacitor. The capacitor is connected in parallel with the load as shown in Fig. 6. Fig. 7 depicts the waveforms obtained at 3000 rpm with C_{dc} = 20 mF and R_{dc} = 0.75 ohm.

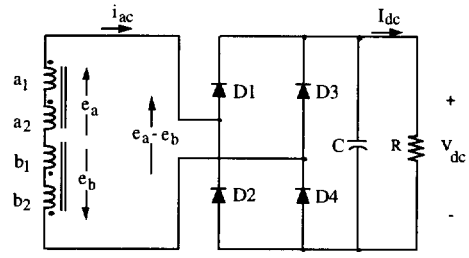

Fig. 6 Rectification with constant dc current.

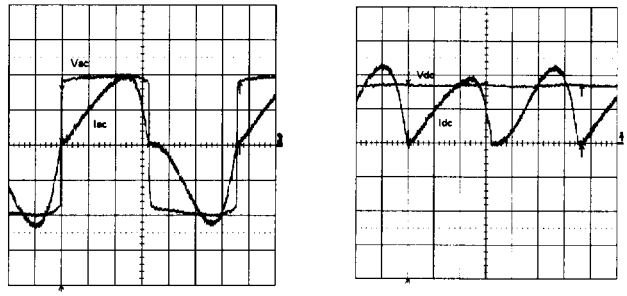

Fig. 7 **Left:** AC output voltage (10 V/div) and AC output current (20A/div) of the DSPM generator **Right:** DC load voltage (10 V/div) and DC load current (20A/div) of the DSPM generator

A. Output Characteristic Of Generator

Various tests are completed for a variety of load values with C_{dc}=20 mF. Fig. 8 and Fig. 9 shows the dc output relationships. As the generator is loaded, the dc voltages again decrease while the dc power output peaks roughly 30 A.

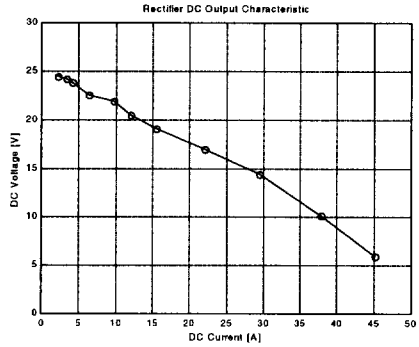

Fig. 8 DC current and DC voltage characteristic

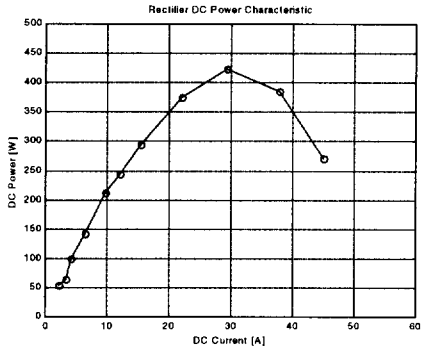

Fig. 9 DC current and DC power characteristic

B. Comparison of Experimental Results with Simulations

Experimental results are compared with the nonlinear and first order approximation simulations. Results are tabulated in Table 2. 3.5 V diode voltage drop is included in the simulations. As can be seen, the first order approximation simulation overestimates the power production capability by about 20 percent due to the simplified inductance and back emf voltage modeling. However, nonlinear simulation provides better accuracy as in the case of rectifier with constant dc link current.

TABLE II
COMPARISON OF EXPERIMENTAL, NONLINEAR SIMULATION, AND FIRST ORDER APPROXIMATION RESULTS.

Results From	DC Output Power (W)	DC Output Power (pu)
Experiment	1400	1.00
Nonlinear Sim.	1320	0.94
First Order App. Sim.	1710	1.22

IV. BOOST CONVERTER WITH HYSTERESIS CURRENT CONTROLLER

The ac output of the DSPM generator can also be rectified by a boost converter utilizing a hysteresis current controller. A hysteresis controller was designed and built for this purpose. The test setup includes the prototype DSPM generator, the power electronics converter, gate drives, and hysteresis current controller. The schematic of implementation of the boost converter with hysteresis current controller is shown in Fig. 10.

The converter has two Insulated Gate Bipolar Transistors (IGBTs) and two diodes. The control circuitry includes the generation of a reference signal, a hysteresis controller, and blanking circuits for IGBTs. A disk is mounted on the rotor with two sets of holes, and two position sensors are used to detect the rotor position. A variable current reference was generated from the signals obtained from the position sensors. The complementary TTL output signals obtained from the control circuitry with proper blanking time were sent to the IGBT gate drives. One LEM current sensor was used to measure the instantaneous phase current.

The DSPM generator was run powered by a separately excited dc machine, and the field current was kept constant while the armature voltage was changed for speed control. The torque on the shaft is measured via a torquemeter, and the signal was smoothed by a low pass filter.

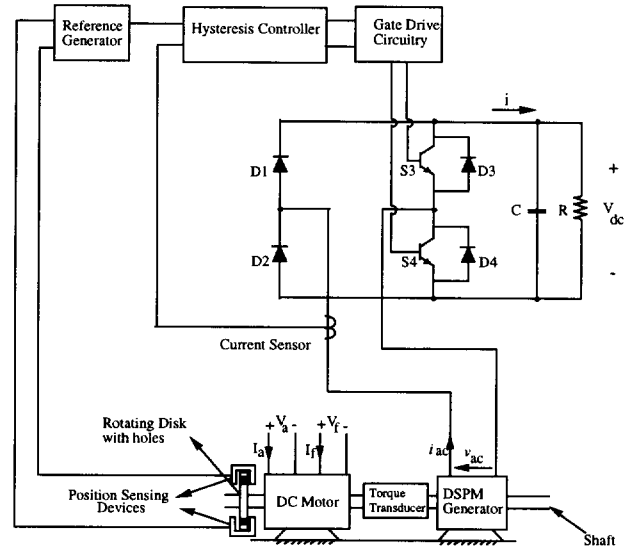

Fig. 10 Schematics of implementation of the boost converter with hysteresis current controller

Fig. 11 shows the low speed results at 870 rpm. It can be observed that the AC voltage is not zero when the machine is short-circuited due to the diode and IGBT voltage drops. From Fig. 11, the output voltage has considerable ripple, since the output capacitor is not sufficiently large. In this case, the output capacitance is 20 mF, paralleled with the load for filtering the dc output voltage.

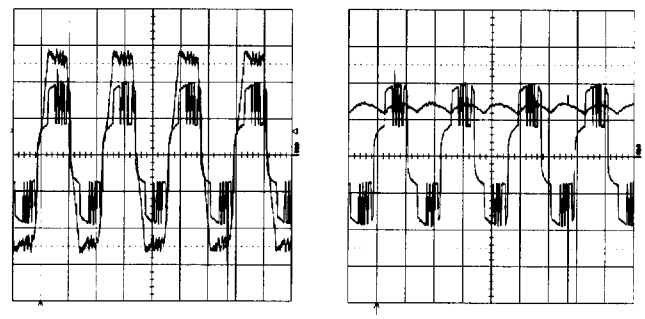

Fig. 11 **Left:** AC current (10 A/div) and AC voltage (4.85 V/div) at 870 RPM, **Right:** DC voltage (5 V/div) and AC voltage (4.85 V/div) at 870 RPM

High speed results at 3000 rpm are illustrated in Fig. 12. Since the torque waveform has high frequency noise, the signal was filtered by a low pass filter. The cutoff frequency of the low filter was placed at 6 kHz. As can be seen, the torque has notches whenever the machine is short-circuited. During this short-circuit, the generated power is stored in the machine inductance and not sent to the load. Therefore, less shaft torque is required in this mode of

operation. However, when the machine is connected to the load, the torque is increased and remains constant. At this point, the energy in the generator inductance and the power taken from the shaft are converted to electrical power at the dc side. The bottom trace of figure on the left shows the reference current and actual current. It can be seen that the measured current tracks the reference current very well. The rise of the actual current to the reference current is slower than when the actual current commanded to zero. This is mainly due to the operating principle of the boost converter. The machine back emf is applied to the machine inductance when one diode and one IGBT are on. A larger voltage, which is the sum of the back emf and the dc output voltage, is applied to the generator inductance, when the two diodes are on and the generator is connected to the load short. As can be seen from figure on the right the output voltage no longer has significant ripple, since the output capacitor is increased to 64 mF from 20 mF. The switching frequency in this case is measured as 2.4 kHz.

The dc output voltage is measured at 35 V and power at the dc side is calculated as 612.5 W when the load is 2 ohms at the dc output. Considering the diode and IGBT drops, the ac power is more than the dc power. If it is noted that the output power of the rectifier with constant dc output voltage at 2 ohms is 220 W, use of the boost converter with a hysteresis controller increases the output power by a factor of nearly three (2.75). This is mainly due to the fact that the output power can be maximized by choosing the optimum current reference. Also the reference can be advanced to attempt to make the voltage and current in phase. From this it can be concluded that a better utilization of the DSPM generator can be obtained by using actively controlled power electronics topologies rather than passive ones.

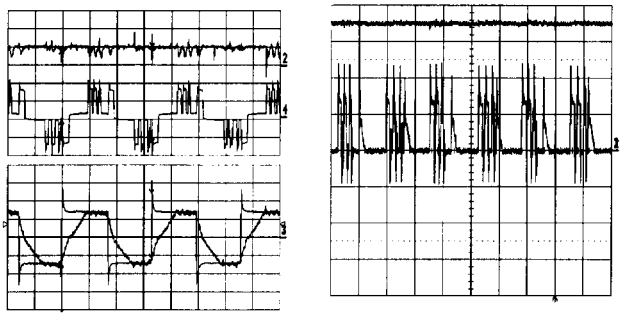

Fig. 12 **Left:** Torque 150 inch-lbs/V, AC voltage (25 V/div) (moved down by 1.8 divisions for clarity of illustration), Current reference (50A/div), Current (50A/div) at 3000RPM **Right:** DC voltage (10 V/div) and DC current (50 A/div) at 3000 RPM

V. CONCLUSION

In this paper, the problem of deriving dc power from a DPSM generator through typical bridge rectifiers and a boost converter with hysteresis controller has been presented. It has been shown that the rectifiers with constant dc voltage and constant dc current can be used for transferring ac power of the DSPM generator to dc power. Use of a rectifier with constant dc voltage produces 30 % more power than a rectifier with constant dc current at the same load. Also, a boost converter with hysteresis controller is designed for converting ac to dc power. More power output is obtained by using a boost converter than using diode bridge rectifiers. In this topology, power conversion can be controlled actively by changing the magnitude and phase of the current reference.

The experimental results are also compared with first order approximation and nonlinear simulations. The nonlinear simulation results are shown to provide better accuracy than the first order approximation simulation.

While it can be concluded that diode bridge rectifiers are preferred for inexpensive and simple power conversion, actively controlled converters better utilize the power capability of the DSPM generator at the expense of increased complexity and cost.

VI. ACKNOWLEDGMENT

Wisconsin Electrical Machine and Power Electronics Consortium (WEMPEC) is gratefully acknowledged for funding this project. Thanks are also given to the Miller Electric Company for construction of the generator.

REFERENCES

[1] Sarlioglu, B., Zhao, Y., Lipo, T.A., "A Novel Doubly Salient Single Phase Permanent Generator", *IEEE IAS Annual Meeting*, Denver, CO, Oct. 2-6, 1994, pp. 9-15.

[2] Sarlioglu, B., Lipo, T.A., "Comparison of Power Production Capability Between Doubly Salient Permanent Magnet and Variable Reluctance Type Generators", *1995 Aegean Conference on Electrical Machines and Power Electronics*, Kusadasi, Turkey, June, 1995.

[3] Lipo, T.A., Li, Y., Luo, X., Sarlioglu, B., "Doubly Salient Permanent Magnet Machines- A Progress Report", *International Symposium on Electric Power Engineering*, Stockholm, June 18-22, 1995.

[4] Sarlioglu, B. and Lipo, T.A., "Nonlinear Modeling and Simulation of Single Phase Doubly Salient Permanent Magnet Generator", *IEEE IAS Annual Meeting*, St. Louis, MO, Oct. 12-15, 1998.

[5] Liao, Y., Liang, F., and Lipo, T.A., "A Novel Permanent Magnet Motor with Doubly Salient Structure", *IEEE IAS Annual Meeting*, Houston TX, Oct. 5-8, 1992, pp. 308-314.

[6] Shakal, A., Liao, Y., Lipo, T.A., "A New Permanent Magnet Motor Structure with True Field Weakening", *IEEE International Symposium on Industrial Electronics*, Budapest, Hungary, June 1993, pp. 19-24.

[7] Liao, Y. and Lipo, T.A., "Sizing and Optimal Design of Doubly Salient Permanent Magnet Motors", *IEE 6th International Conference on Electrical Machines and Drives*, Sept. 8-10, 1993, pp. 452-456.

APPENDIX

The photo shown in Fig. A.1 illustrates experimental arrangement for the boost converter.

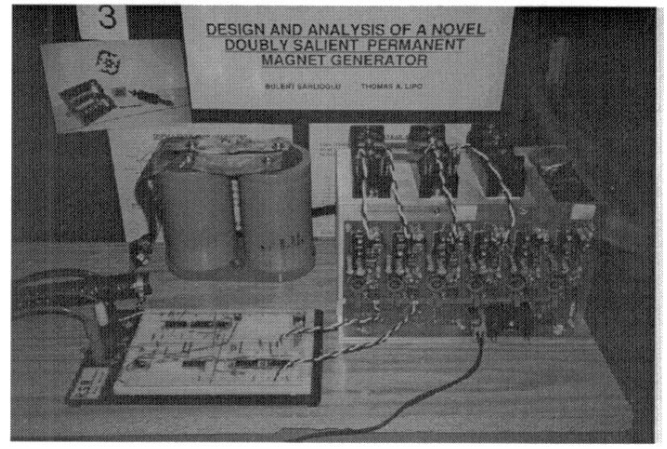

Fig. A.1 The boost converter with hysteresis controller